ChemComm

FEATURE ARTICLE

View Article Online
View Journal

Cite this: DOI: 10.1039/c6cc05581h

Functionalized carbon nanotubes and graphene-based materials for energy storage

Bin Wang,[ab] Chuangang Hu[a] and Liming Dai*[a]

Received 6th July 2016,
Accepted 7th September 2016

DOI: 10.1039/c6cc05581h

www.rsc.org/chemcomm

Carbon nanotubes (CNTs) or graphene-based nanomaterials functionalized by different strategies have attracted great attention for energy storage due to their large specific surface area, high conductivity, and good mechanical properties. This feature article presents an overview of the recent progress in the functionalization of CNTs and graphene-based materials for energy storage applications in supercapacitors and batteries, along with challenges and perspectives in this exciting field.

1. Introduction

Supercapacitors (also called as electrochemical capacitors or ultracapacitors) and batteries have been considered as one of the most promising technologies to solve our energy and environmental challenges.[1–5] Supercapacitors can store energy *via* electrostatic charge accumulation at the interface between the electrode surface and the electrolyte, reversible redox reactions (Faradaic processes) occurring on the surface of electrodes, or both.[6] Due to the fast kinetics, characteristic of the charge storage processes, supercapacitors can quickly deliver a power output in a very short time with high power densities, but poor energy densities. On the other hand, batteries store and release energy *via* reversible electrochemical reactions between the cathode and the anode.[7] Compared with supercapacitors, batteries have higher energy density with limited power density due to the nature of energy storage processes involved (Fig. 1).[8] Lithium-ion batteries are normally composed of a graphite-based anode, a lithium transition metal oxide-based cathode, and a carbonate-based organic electrolyte,[9,10] and have been regarded as one of the most attractive batteries for large-scale rechargeable applications because of their high energy density and good electrochemical performance.[9–19] While lithium-ion batteries are currently receiving intensive attention, many other types of batteries, including lithium–sulfur batteries,[20–25] zinc–air,[26–28] lithium–oxygen batteries,[29–35] and sodium-ion batteries,[36] have also been widely investigated.

The overall performance of energy storage devices strongly depends on the structure and properties of the materials used, including electrode materials and electrolytes. In this regard, a large variety of nanostructured materials have been developed for energy storage. Among them, graphitic carbon nanomaterials,

[a] Center of Advanced Science and Engineering for Carbon (Case4Carbon), Department of Macromolecular Science and Engineering, Case Western Reserve University, Cleveland, OH 44106, USA. E-mail: liming.dai@case.edu
[b] Institute of Chemical Materials, China Academy of Engineering Physics, Mianyang, Sichuan, 621900, China

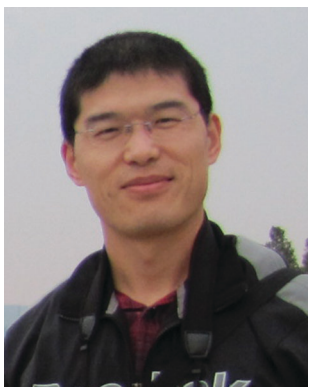

Bin Wang

Bin Wang is a staff scientist in the National Energy Novel Materials Center, Institute of Chemical Materials. He received his PhD degree from Fudan University in 2009. He was a postdoctoral scholar at the Lawrence Berkeley National Lab (LBNL, USA) during 2009–2013 and then joined the National Energy Novel Materials Center. His research focuses on the development and applications of novel materials for energy conversion and storage.

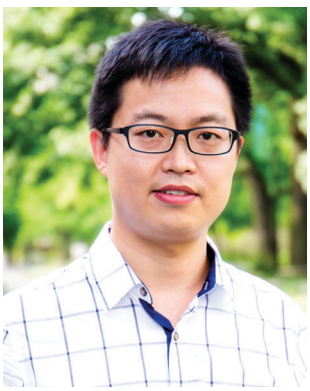

Chuangang Hu

Chuangang Hu received his MS from Henan Normal University in 2011, and his PhD from the Beijing Institute of Technology in 2015. He is currently a post-doctoral research associate in Professor Liming Dai's group at Case Western Reserve University. His research interests focus on carbon-based materials for energy conversion and storage.

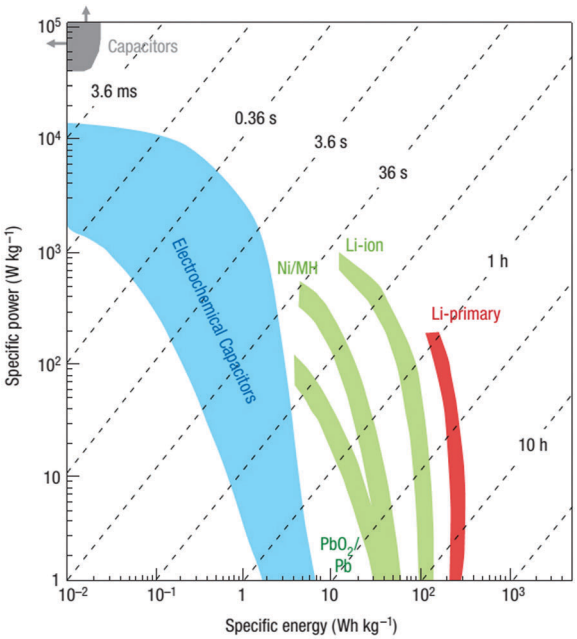

Fig. 1 Ragone plots of various electrical energy storage devices.[8] Reprinted from ref. 8 with permission. Copyright 2008, Nature Publishing Group.

especially carbon nanotubes (CNTs) and graphene nanosheets, have emerged as promising electrode materials for the development of next-generation energy storage devices (Fig. 2).

Traditionally, carbon-based materials, such as activated carbon and graphite, have been used as electrodes for supercapacitors and batteries. However, both the structure and properties of these carbon-based electrodes need to be further improved for high-performance supercapacitors and batteries. Recent development in nanoscience and nanotechnology has opened up new frontiers in materials science and engineering to meet this challenge by creating new materials, particularly carbon nanotubes and graphene, for efficient energy storage.

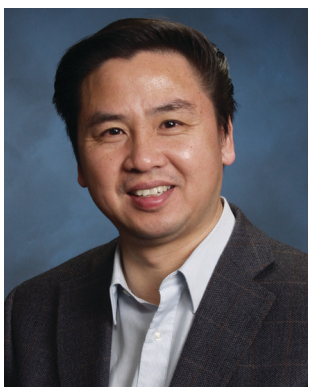

Liming Dai

Liming Dai is a Kent Hale Smith Professor at Case Western Reserve University in the Department of Macromolecular Science and Engineering and is also the director of the Center of Advanced Science and Engineering for Carbon (Case4Carbon). He received a BSc from Zhejiang University in 1983, and a PhD from the Australian National University in 1991. After his post-doctoral research at the Cavendish Laboratory in Cambridge, he spent 10 years with the Commonwealth Scientific and Industrial Research Organization in Australia. Before joining the CWRU in 2009, he was an associate professor of polymer engineering at the University of Akron and the Wright Brothers Institute Endowed Chair Professor of Nanomaterials at the University of Dayton.

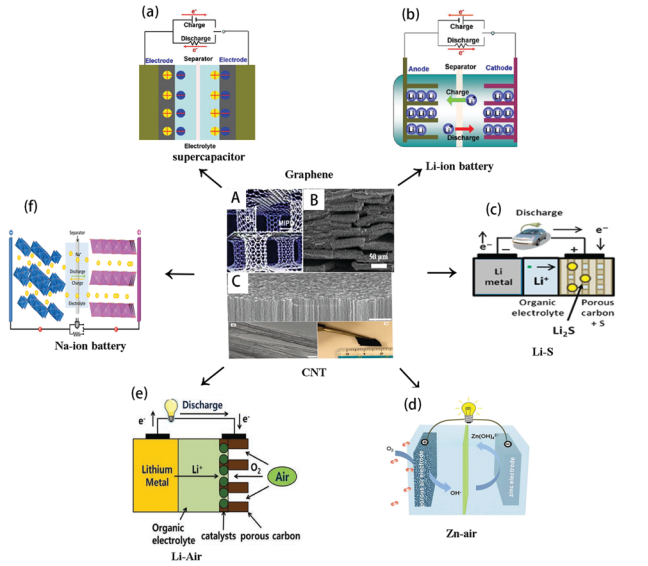

Fig. 2 Schematic diagrams of the CNTs and graphene for energy storage applications. (A and B) Schematic diagram of a 3D pillared VACNT graphene nanostructure and its SEM image. Reprinted from ref. 3 with permission. Copyright 2011, American Chemical Society. (C) Nitrogen-doped VACNTs. Reprinted from ref. 33 with permission. Copyright 2009, AAAS. (a and b) Schematic diagrams of the working principle of a Li-ion battery and a supercapacitor. (c) Schematic diagram of the working principle of a Li–sulfur battery. Reprinted from ref. 34 with permission. Copyright 2011, the Materials Research Society. (d) Schematic diagram of the working principle of a Zn–air battery. Reprinted from ref. 35 with permission. Copyright 2014, the Royal Society of Chemistry. (e) Schematic diagram of the working principle of a Li–air battery. Reprinted from ref. 30 with permission. Copyright 2011, John Wiley and Sons. (f) Schematic diagram of the working principle of a Na-ion battery. Reprinted from ref. 36 with permission. Copyright 2015, John Wiley and Sons.

Since their discovery by Iijima in 1991, CNTs have been widely used as new electrode materials for energy storage devices because of their large specific surface area as well as good electrical and mechanical properties.[3,17,37] Single-walled CNTs (SWCNTs) can be viewed as a graphene sheet, which is rolled up into a nanocylinder,[38] while multi-walled CNTs can be formed by coaxially rolling up multilayer graphene sheets. Depending on the wall number, chiral vector, defect type and number, nanotube diameter and its length, the electrical conductivity of CNTs varies from insulating, through semiconducting, to metallic conducting. CNTs can be prepared by various synthesis methods, including chemical vapor deposition (CVD), ball-milling, the radio-frequency induction thermal plasma method, and arc-discharge.[3,39–41] Of particular interest, vertically aligned CNTs (VACNTs) have also been synthesized by many groups in recent years.[39,42–47] Due to the well-defined structure (*e.g.*, nanotube length, diameter) and high purity intrinsically associated with the vertical growth, VACNTs show great promise for a wide range of potential applications. While the energy-related applications will be discussed in succeeding sections, as appropriate, readers who are interested in more potential applications of VACNTs are referred to some excellent review articles

published previously.[17,39,41,48–50] However, the as-synthesized CNTs without functionalization are easy to aggregate, insoluble and infusible, limiting their applications in many fields. Furthermore, pristine CNTs are difficult to be integrated with other functional materials, such as metal oxides[51–53] and noble metals,[54] to generate any possible synergistic effect. For practical applications, therefore, it is highly desirable to develop functionalized CNTs with controllable surface characteristics, physicochemical properties, and processability.

Graphene, the one-atom-thick planar sheet of sp^2-bonded carbon atoms, has many similarities in structure and properties to CNTs. The discovery of graphene by Andre Geim and Konstantin Novoselov was recognized by a Nobel Prize for Physics in 2010.[55,56] Due to its large specific surface area (2630 $m^2 g^{-1}$), high aspect ratio (the ratio of lateral size to thickness), low density, high carrier mobility for both the electron and holes, and excellent mechanical properties, graphene has shown tremendous potential for various applications, including energy storage.[1,5,11,57,58] The availability of many rational strategies for covalent functionalization and noncovalent functionalization of graphene and CNTs could modulate the properties and processability of CNTs and graphene-based materials for energy storage applications, as described below. In this article, we summarize the rational design and development of functionalized CNTs and graphene-based materials for efficient energy storage devices (*e.g.*, supercapacitors and batteries), along with some remarks on challenges and perspectives in this exciting field. Since this feature article focuses on our own work, examples to be presented below will undoubtedly not include all significant work reported in the literature.

2. Functionalization of CNTs and graphene-based materials

Through chemical oxidation of CNTs and graphene materials, oxygen-containing covalent functional groups (*e.g.*, hydroxyl, carbonyl, and carboxylic acids) can be introduced into the nanocarbon structure, which can be used for further functionalization.[58,59] In addition to chemical oxidation, there are several other functionalization possibilities for CNTs and graphene at both molecular and supramolecular levels, including covalent grafting and noncovalent assembling with polymer chains or surfactants, as shown in Fig. 3. The covalent functionalization could significantly change the electrical structure and properties of the CNTs and graphene whereas the noncovalent functionalization, *via* the weak interaction of van der Waals, π–π interactions and electrostatic force, would maintain the chemical structure and physical properties of the CNTs and graphene to a great extent. In particular, acid (*e.g.*, nitric acid or sulfuric acid) oxidation is one of the most commonly used methods for covalent functionalization while the noncovalent functionalization through physical adsorption of aromatic compounds or polymer chains has been widely reported.[51–53,60] Of particular interest, Cheng *et al.* developed a simple and green noncovalent functionalization through π–π interaction by using CNTs as a shape template and

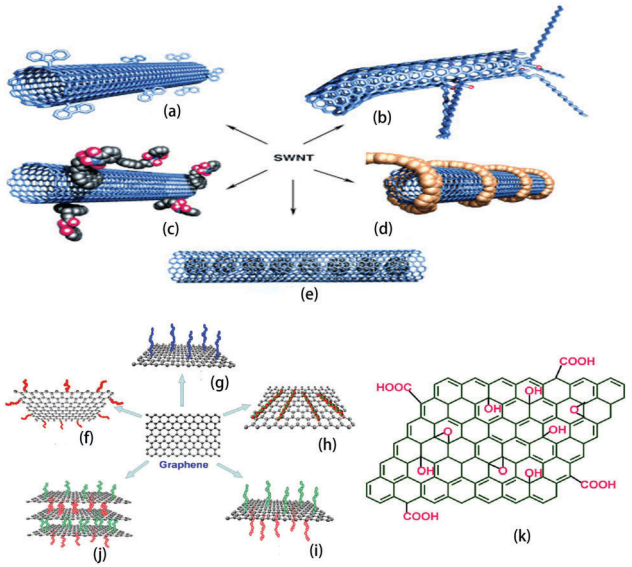

Fig. 3 (a–e) Functionalization possibilities for SWCNTs: (a) covalent sidewall functionalization, (b) defect-group functionalization, (c) noncovalent exohedral functionalization with surfactants, (d) noncovalent exohedral functionalization with polymers, and (e) endohedral functionalization with, for example, C_{60}. For methods a–e, the tubes are drawn in an idealized fashion, but defects are found in real situations. Reprinted from ref. 68 with permission. Copyright 2002, John Wiley and Sons. (f–k) Functionalization possibilities for graphene: (f) edge-functionalization, (g) basal-plane-functionalization, (h) noncovalent adsorption on the basal plane, (i) asymmetrical functionalization of the basal plane, and (j) self-assembling of functionalized graphene sheets. (k) Chemical structure of graphene oxide.[1] Reprinted from ref. 1 with permission. Copyright 2013, American Chemical Society.

glucose grafted with aromatic compounds as a structure-directing agent without involving any pre-treatment or any surfactant/ligand.[53] The attached glucose with multiple hydroxyl groups can act as a bridge to connect metal oxides (Fig. 4). This noncovalent functionalization method is general and can also be used for other metal oxides[12,51] and applied to graphene-based materials.[12]

Different functionalized CNTs and graphene materials have been reported to possess novel properties for multifunctional applications, including new electrode materials in energy

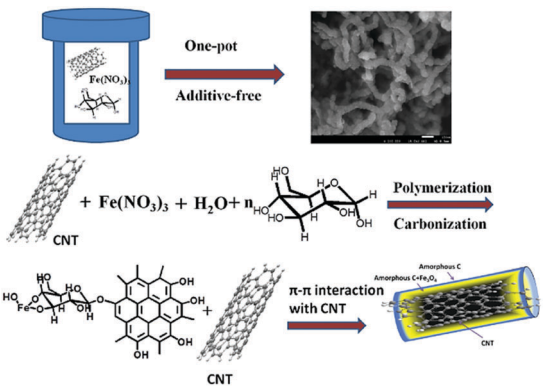

Fig. 4 π–π interactions used for the synthesis of the CNT@Fe_3O_4@C nanocable. Reprinted from ref. 53 with permission. Copyright 2013, John Wiley and Sons.

storage devices. For instance, epoxidation-functionalized CNTs with stretch alignment have been used to reinforce bismaleimide resin, which exhibited an unprecedentedly high tensile strength of 3081 MPa and a modulus of 350 GPa well exceeding those of the state-of-the-art aerospace-grade randomly oriented carbon–fiber composites.[61] Ionic liquid-functionalized partially exfoliated multiwalled CNTs (MWCNTs) have been prepared by oxidation of MWCNTs[62] as matrices for electropolymerized pyrene derivatives. The resultant composites showed a maximum mass-specific electrochemical activity through electrostatic interaction between the oxygen functionalities and protonated amino groups.[63] Phosphate-functionalized CNTs have been prepared by a one-pot soft-template hydrothermal reaction of copolymers, CNTs, fructose, and H_3PO_4, followed by heat treatment, as high-performance electrodes in supercapacitors.[64] N-doped VACNTs and graphene-based materials have also been reported as metal-free catalysts for the oxygen reduction reaction (ORR) in fuel cells with a three times higher electrocatalytic activity and better long-term stability than those of commercial Pt/C electrodes[65,66] as well as high-performance metal–air batteries.[28,67]

Besides, Du *et al.* designed tunable 3D pillared VACNT–graphene architectures through the intercalated growth of VACNTs, *via* pyrolysis of FePc, into thermally expanded highly ordered pyrolytic graphite (HOPG), from which high-performance supercapacitors with high rate capability and excellent cycling ability.[3] Zhang *et al.* grew N, Fe, Co-doped CNTs on the skeleton of 3D nitrogen-doped carbon foams to show high electrochemical stability.[69] Similarly, functional CNTs have been incorporated with other components, including polyethyleneimine,[70] metal catalysts,[71,72] vanadium nitride,[73] pyrrole[74] and polythiophene[75] for various energy-related applications. By functionalizing with different functional groups, the CNTs can possess distinctly different properties, which would help to achieve and broaden new applications of the CNTs.

For graphene, both sides of its basal plane can be functionalized with the same moieties (symmetrical functionalization) or different functional groups (asymmetrical functionalization) (Fig. 3g–j). Just like functionalized CNTs, covalent functionalization on the graphene basal plane could cause significant changes in its structure and properties while noncovalent functionalization through weak physical interactions can well retain the properties of graphene. Liu *et al.* and Yu *et al.* performed controlled edge/basal-plane selective functionalization of graphene/graphene oxide, and the edge-functionalization could change the work function of graphene oxide to produce excellent charge transport/extraction materials for solar cells.[76,77] On the other hand, the substitution of the epoxy and/or hydroxyl groups on the basal plane of graphene oxide with $-OSO_3H$ groups can lead to an excellent hole extraction material with improved solubility, and hence film formability.[78] Moreover, attaching C_{60} onto a graphene sheet could provide all-carbon composite materials as good electron transporting or accepting materials.[79] In addition to the above chemical functionalizations, doping of graphene with heteroatoms, such as N,[2,65,80] B,[81] S,[82,83] and P,[84] could produce multifunctional carbon-based materials for energy storage applications (*e.g.*, supercapacitors, batteries) and beyond (*e.g.*, fuel cells, solar cells).[67]

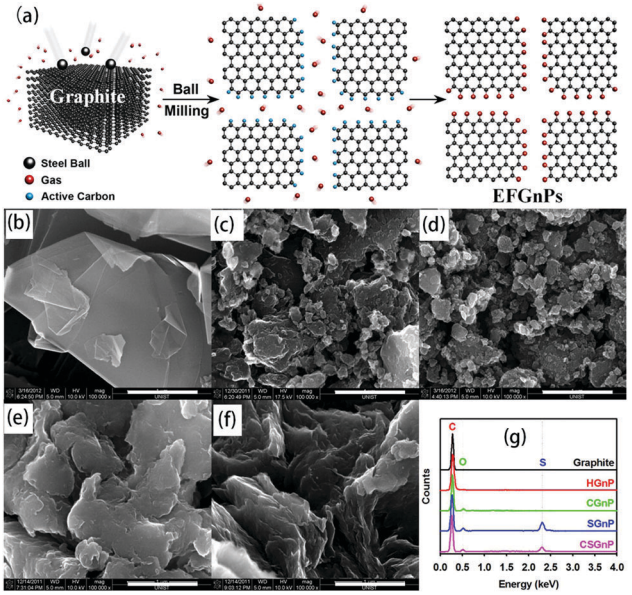

Fig. 5 Edge-selectively functionalized graphene nanoplatelets with different functional groups were efficiently prepared simply by dry ball milling graphite. Reprinted from ref. 86 with permission. Copyright 2013, American Chemical Society.

Edge functionalized graphene nanoplatelets (GnPs) have also been produced by ball milling at a relatively low cost and large scale (Fig. 5).[85–89] Specifically, GnPs functionalized with different edge-groups, such as hydrogen-(HGnP),[86] carboxylic acid-(CGnP),[85] sulfonic acid-(SGnP),[86] carboxylic acid/sulfonic acid-(CSGnP),[86] nitrogen (NGnPs),[80,88] fluorine (FGnPs),[11] XGnP (X = I, Br, Cl),[89] and sulfur GnP,[82] have been prepared and used for energy conversion and storage.[90] The properties of the edge functionalized groups can directly affect the electrocatalytic-activity and/or chemical-reactivity characteristics of the composites with the well retained properties of graphene. The edge functionalization of graphene by ball-milling is scalable and efficient, which would be quite helpful for large-scale applications.

3. Functionalized CNTs and graphene-based materials for supercapacitors and batteries

As mentioned above, supercapacitors and batteries are the main energy storage devices. In order to meet their increasing demand for applications, such as large-scale electric vehicles, the performances of existing supercapacitors and batteries, including their specific capacity, energy density, power density, durability, and safety, need to be further improved. Due to their unique electrical and mechanical properties, CNTs and graphene-based materials, with and without functionalization, have attracted particular interest for energy applications.

3.1 Functionalized CNTs and graphene-based materials for supercapacitors

As is well known, activated carbon materials have been widely used as electrode materials in supercapacitors. However, their high surface area and a relatively low mesoporous structure have led to low electrolyte accessibility, and thus limited energy density (4–5 W h kg^{-1}) and power density (1–2 kW kg^{-1}).[91] In order to improve the capacitance and energy density, various CNTs and graphene-based materials functionalized with or without metal oxides or polymers have been used as the current collector or electrode materials in supercapacitors. In this context, Yu *et al.* used the layer-by-layer (LBL) approach to self-assemble cationic poly(ethyleneimine) polymer-modified graphene sheets and acid-oxidized multi-walled CNTs into multi-layered graphene–polymer composites.[92] The obtained hybrid films possess a good carbon interconnected network with well-defined nanopores, which can deliver a specific capacitance of 120 F g^{-1} at a high scan rate of 1 V s^{-1}. Jiang *et al.* reported that an asymmetric supercapacitor, consisting of birnessite-type ultrathin porous MnO_2 nanoflowers as the positive electrode and functional mesoporous CNTs as the negative electrode and 1 M Na_2SO_4 solution as the electrolyte, can exhibit a maximum specific capacitance of 85.8 F g^{-1} with a high energy density of 47.4 W h kg^{-1} at a power density of 200 W kg^{-1}, superior cycling stability (90% retention after 1000 cycles), and high Coulombic efficiency.[93] Guan *et al.* prepared a graphene and needle-like cobalt oxide (CoO and Co_3O_4) composite by the hydrothermal method. When used as electrode materials for aqueous supercapacitors, the resultant composites exhibited a high specific capacitance of 157.7 F g^{-1} at a current density of 0.1 A g^{-1} and a 70% retention after 4000 cycles.[94]

Furthermore, Zheng *et al.* developed a low-cost and highly scalable approach to fabricate supercapacitors based on multi-layered graphene with a high proportion of the edge structure by directly drawing graphite on a piece of cellulose paper. The paper supercapacitor thus produced showed a stable high areal capacitance of 2.3 mF cm^{-2} (23 F g^{-1}), which is much higher than that of the corresponding data previously reported (Fig. 6).[95] With the redox metal oxide or polymer in the electrode, the energy density can be further enhanced. Similarly, supercapacitors based on CNTs and graphene-based materials integrated with various metal oxides or polymers, such as Co_3O_4–rGO/CNTs,[98] MnO_2–CNTs,[93,99] $Ni(OH)_2$–CNT–graphene,[3] CNT–graphene,[92] and CNT–rGO–PANI,[106] have also been prepared and are summarized in Table 1. It can be seen that the performances of the supercapacitor, especially the energy density and specific capacitance, have greatly improved with various functionalized CNTs and graphene based materials.[107] It should also be noted that the stability and energy density of the redox reaction-based electrode of the supercapacitor still need to be further improved for practical device applications.

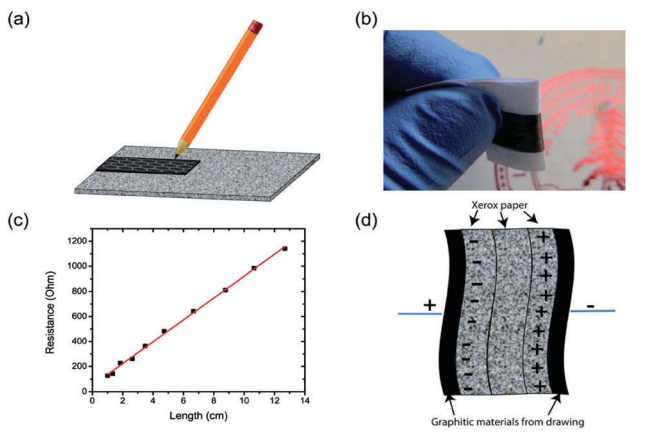

Fig. 6 (a) Schematic diagram of drawing a conductive electrode on cellulose paper using a graphite pencil. (b) Digital camera image showing the finished conductive paper electrode from drawing. (c) Resistance measurement of the graphitic coating on paper (width of the graphite stripe is 2.0 cm) over different lengths. (d) Schematic diagram of the paper supercapacitor device. Reprinted from ref. 95 with permission. Copyright 2011, the Royal Society of Chemistry.

Compared with randomly entangled CNTs, VACNTs can not only provide a larger specific surface area but also can facilitate the electron/electrolyte transport, leading to improved electrochemical performance.[91,96,108,110–112] The top end-caps of VACNTs can even be opened by plasma etching to expose the nanotube inner-wall for charge storage,[91] which, in conjunction with ionic liquids as the electrolyte, can lead to a cell voltage as high as 4 V, an energy density of 148 W h kg^{-1}, and a power density of 315 kW kg^{-1}.[91] So the supercapacitor with high energy density and reasonable power density might be obtained by combining the highly capacitive behavior of VACNT electrodes with the large electrochemical window of ionic liquid electrolytes. With further improved conductivity, the ionic liquid has potential to outperform the current electrochemical capacitor technology.

Recently, high-performance flexible, stretchable, and even transparent supercapacitors have been developed by using polymer-supported CNT thin film electrodes (Fig. 7a–e and j–t),[108,109] 3D graphene–CNT pillar electrodes (Fig. 7f–i),[3] and fiber-shaped CNT-wrapped polymer electrodes (Fig. 7u–x).[103] For developing the next generation energy devices, transparent and/or stretchable energy storage devices are highly in demand due to their unique optical and/or mechanical properties as well as their intrinsic energy storage function.

Chen *et al.*[103] developed wrinkled graphene sheets that can be used as both current collectors and electrode materials to fabricate transparent and stretchable supercapacitors, which can have high transparency (57% at 550 nm) and be stretched up to 40% strain without an obvious performance change over hundreds of stretching cycles. This study provides a novel strategy to develop highly transparent and stretchable all-solid supercapacitors useful for a large variety of potential applications. Although graphene sheets have a large specific surface area, the strong interlayer π–π stacking caused the loss of a significant portion of the graphene surface area and active sites for energy storage.

Du *et al.* developed a 3D graphene–CNT nanopillar (Fig. 7f–i) with alternating graphene and VACNT layers, which allows for graphene layers to be separated by VACNT arrays, thus showing a high specific capacitance and remarkable rate capability.[3,110]

Table 1 Summary of the morphology, synthesis conditions, and subsequent specific capacitance of CNT/graphene based materials

Component	Synthesis conditions	Electrolyte	Capacitance	Ref.
Multilayer graphene	Hand drawing	1 M H_2SO_4	23 (0.2) F	95
Titania and CNTs	Hand wrapping	PVA–H_3PO_4	1.84 MF	96
MnO_2–CNTs	Hard template	1 M Na_2SO_4	85.8 F	93
3D graphene Co_3O_4	CVD	2.0 M KOH	1100 (10) F	97
Co_3O_4–rGO/CNTs	Hydrothermal method	3 M KOH	378 (2) F	98
Co_3O_4–graphene	Hydrothermal method	2 mol L^{-1} KOH	157.7 (0.1) F	94
MnO_2–CNTs	Vacuum-filtering	PVA/LiCl	29.3 (0.5) MF	99
CNT–PANI	Layer by layer	PVA/H_3PO_4	111.6 (0.5) F	100
CNT–mesoporous carbon	Drop-coating	PVA/H_2SO_4	507.02 (0.87) MF	101
VACNTs/CNFs	CVD	$EMIMBF_4$ ionic liquid	146.8 (0.5) F	102
Wrinkled graphene	CVD	PVA/H_3PO_4	7.6 F	103
GNS–FWCNTs	Solution spinning	PVA–H_3PO_4	38.8 F cm^{-3} (50 mA cm^{-3})	104
$Ni(OH)_2$–CNT–graphene	CVD	0.2 M $Ni(NO_3)_2$	1065 (22.1) F	3
CNT–graphene	Self-assembly	1 M H_2SO_4	120 F g^{-1} (1 V s^{-1})	92
Graphene	CVD	PVA/H_2SO_4	141.2 (1) F	105
rGO–PANI	Solution mixing	1 M H_2SO_4	250 F g^{-1} (0.1 V s^{-1})	106
VACNTs	CVD	PVA/H_3PO_4	7.3 (0.25) F	108
VACNTs	CVD	PVA/H_3PO_4	8.0 (0.5) F	109
3D graphene	CVD	PVA/H_2SO_4	3.33 (2.12) MF	110

Note: poly(vinyl alcohol): PVA, polyaniline: PANI, few walled CNTs: FWCNTs, F g^{-1} (at A g^{-1}): F, mF cm^{-2} (at mA cm^{-2}): MF.

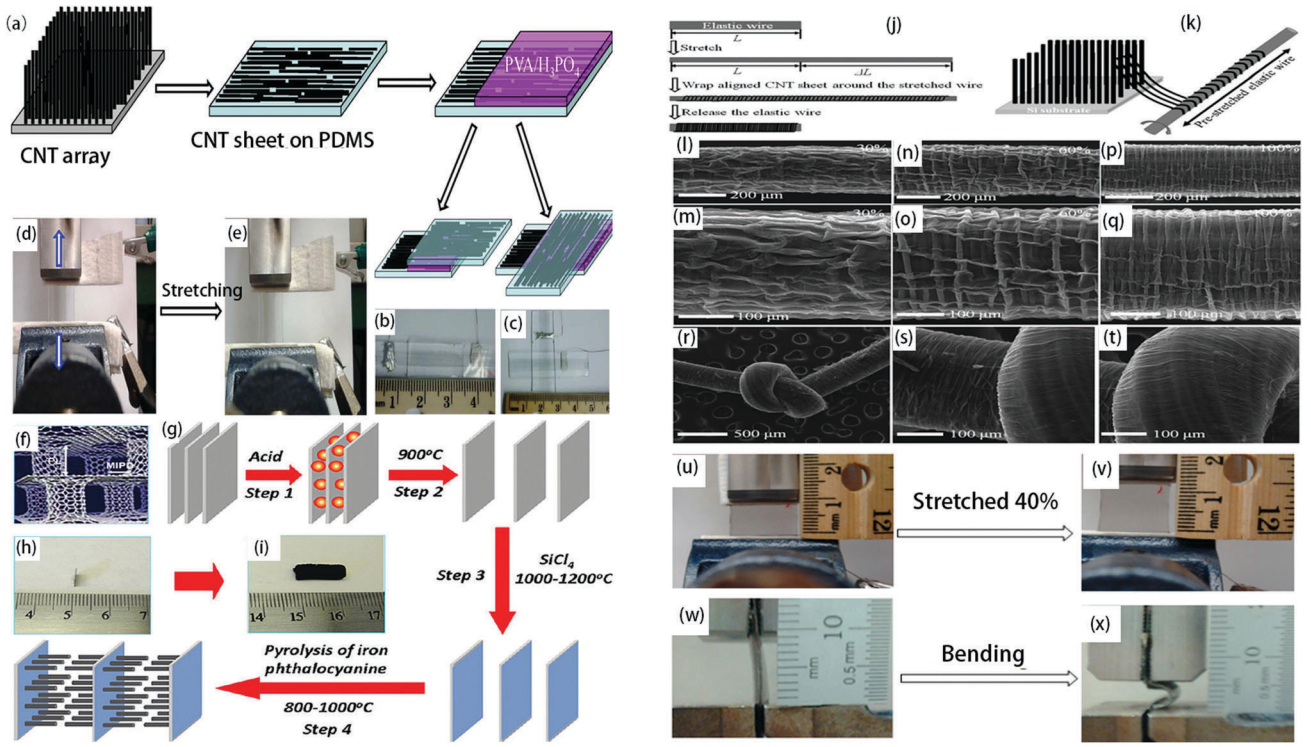

Fig. 7 (a–d) Schematics of the fabrication process for the transparent supercapacitors and their optical images. (a) Schematic of the process for fabricating the transparent and stretchable supercapacitor. (b and c) Photographs of supercapacitors. (d and e) Photographs of a supercapacitor before and after stretching. Reprinted from ref. 108 with permission. Copyright 2014, Nature Publishing Group. (f–i) Schematic diagram of a 3D pillared VACNT graphene nanostructure. (g) Schematic of the procedure for the preparation. Optical images of (h) original HOPG and (i) the graphene nanotubes. Reprinted from ref. 3 with permission. Copyright 2011, American Chemical Society. (j and k) Schematic of fabricating a stretchable conducting wire, SEM images of the CNTs wrapped on a wire with a 30% (l and m), 60% (n and o), and 100% (p and q) pre-strain. (r–t) SEM images of the wire with 100% pre-strain. Reprinted from ref. 109 with permission. Copyright 2015, John Wiley and Sons. (u–x) Stretchability and flexibility of the transparent supercapacitors based on the wrinkled graphene sheets. (u and v) Digital photographs of the supercapacitors before (u) and after (v) being stretched. (w and x) Digital photographs of the supercapacitors before (w) and after (x) being bent. Reprinted from ref. 103 with permission. Copyright 2014, American Chemical Society.

To meet the demand for future wearable energy storage, lightweight, flexible, and wearable supercapacitors have also been reported recently, as exemplified by Fig. 7u–x.[109]

As mentioned above, CNTs and graphene have superior thermal, electrical, and mechanical properties. However, these nanomaterials exhibit poor out-of-plane properties due to the

weak van der Waals interaction in the transverse direction between graphitic layers. Xue *et al.* designed 3D graphene–CNT hollow fibers with radially aligned CNTs seamlessly sheathed by a cylindrical graphene layer through one-step chemical vapor deposition. These fibers have a controllable surface area, meso-/micropores, and superior electrical properties, and so they can be used as good electrode materials for all-solid-state wire-shaped supercapacitors. The corresponding fiber-shaped supercapacitor can deliver a surface-specific capacitance of 89.4 mF cm^{-2} and a length-specific capacitance up to 23.9 mF cm^{-1}, several times the corresponding record-high capacities reported for other fiber-like supercapacitors. It is worth noting that these novel fiber-shaped graphene–RACNT energy conversion and storage devices have good flexibility and mechanical properties, so they have the potential to be used in integrated fabric power sources. Very recently, Li *et al.* has also developed a novel flexible all-solid-state fiber supercapacitor by using Ti/TiO_2/MoS_2 coaxial fiber electrodes (Fig. 8),[113] which exhibited an energy density of 2.70 W h kg^{-1} and a power density of 530.9 W kg^{-1} and could be fabricated into a spring-shaped device, knitted into fabrics (Fig. 8a–e), and integrated into sustainable self-sufficient sensor networks (*e.g.*, a self-powered photodetecting system and as a power source for an ultraviolet photodetector, Fig. 8f–i). It is a good demo for the integrated devices of energy conversion, energy storage, and energy supply.

3.2 Functionalized CNTs and graphene-based materials for batteries

Apart from supercapacitors, batteries, such as lithium-ion batteries,[9,11–13,51–53,89,114,115] sodium-ion batteries,[80,82] lithium–sulfur batteries,[23,24,82,116] lithium–air batteries,[67] and zinc–air batteries,[28] are another important class of energy storage devices due to their high energy densities.

Just like CNT-/graphene-based electrodes in supercapacitors, functionalized CNT- and graphene-based electrodes have also been investigated in various batteries. Recently, Wang *et al.* reported a non-covalent process to coat CNTs with TiO_2 by using glucose as the surfactant.[51] The use of glucose in the hydrothermal process can solve the interfacial incompatibility between CNTs and titanate sol, control the nucleation and growth of TiO_2 particles, and introduce a uniform, glucose-derived carbon-layer on TiO_2 particles. When used as an anode in lithium-ion batteries, the resultant mesoporous CNT@TiO_2-C composite of a well-defined electronically conducting network (inner CNT core and outer carbon layer) coated with fine anatase TiO_2 particles (less than 8 nm) exhibited extremely high rate capability and rate cycling stability as well as a capacity retention of 87% after 2000 cycles at 50 °C.

Recently, edge-fluorinated graphene nanoplatelets (FGnPs) have also been investigated as the electrode materials for Li-ion batteries. With the highest electronegativity of fluorine atoms and the strongest single covalent bond at the edges, FGnPs were demonstrated to show a superb electrochemical performance in LIBs with a high discharge capability of 1778.1 mA h g^{-1} at 0.1 C.[11] Besides, Xu *et al.* used N-doped holey graphene as the electrode material for a Li-ion battery, and demonstrated a high

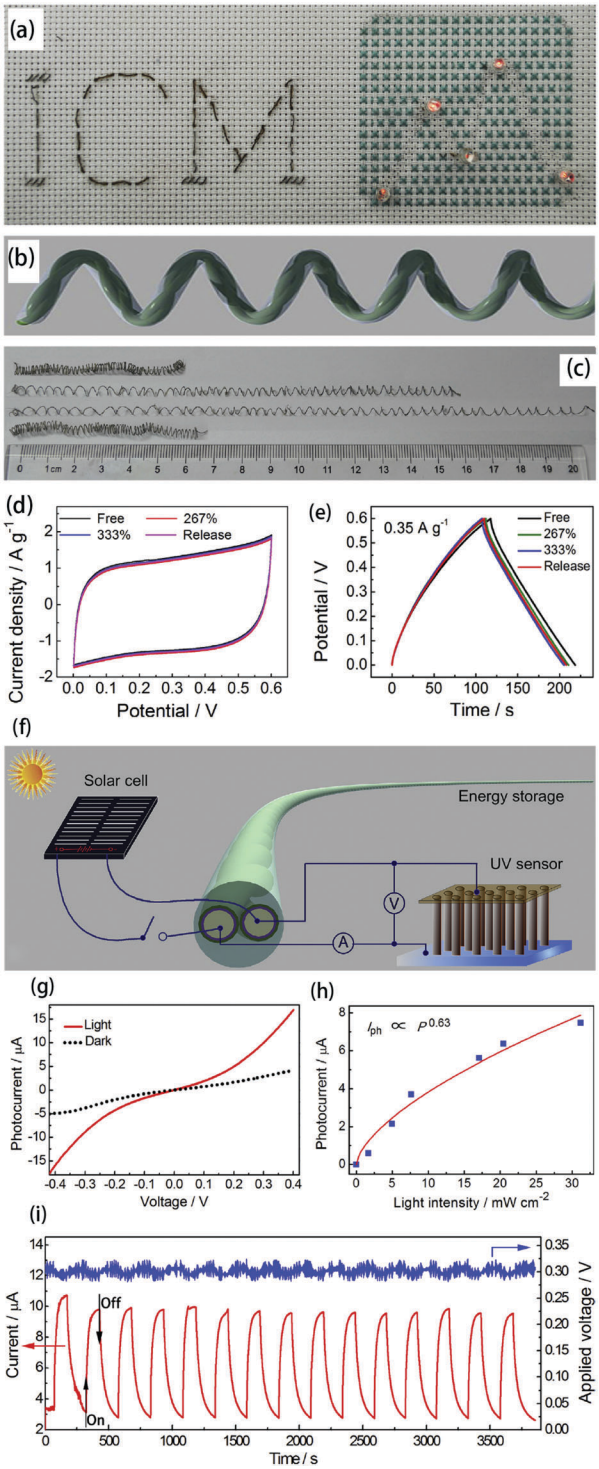

Fig. 8 (a) Digital images of abbreviation and the embroidery logo of the Institute of Chemical Materials (ICM) fabricated from the solid state fiber supercapacitors. (b) Schematic of the spring-like supercapacitors. (c) Photos of the spring-like supercapacitor at different status. (d and e) Show the corresponding CV and GCD curves of the spring-like supercapacitors at free, stretched (267%, 333%) and released status. (f) Schematic of a self-powered system consisting of an energy harvester (solar cell), energy storage (fiber supercapacitors) and a functional nanodevice (UV photodetector). (g) Current (*I*)–voltage (*V*) characteristics of an UV photodetector based on the TiO_2 nanowire array. (h) Photocurrent (I_{ph}) of the UV photodetector. (i) A transient current response of the UV photodetector powered by the solar cell charged fiber supercapacitors. Reprinted from ref. 113 with permission. Copyright 2016, Elsevier B.V.

volumetric capacity of 384 mA h cm^{-3} at 0.1 A g^{-1} and a maximum volumetric energy density of 171.2 W h L^{-1}, which outperformed traditional graphene materials, N-doped graphene, and holey graphene without N-doping.[114] These good electrochemical performances can be attributed to the high electrical conductivity originating from nitrogen doping and holes in the graphene, more active sites for lithium storage and reduced ion diffusion distance stemmed from high packing density and hole structure, and low charge-transfer resistance between the electrolyte–electrode interface. This work indicates that N-doped holey graphene with a high packing density and excellent ion transport/storage properties can serve as promising anode materials with both high gravimetric and volumetric energy densities and long-term cycling stability. These results clearly indicate that edge or surface functionalization has great potential to improve the performances of next-generation of high-performance lithium-ion batteries. Meanwhile, the restacking (or agglomeration) of the graphene sheets is still a challenge for future battery applications because of their severely decreased effective surface area and associated properties.

More recently, a low-cost and scalable approach has been developed to prepare 3D mesoporous carbon foams co-doped with N and P (NPMCs) by pyrolyzing polyaniline aerogels generated from template-free polymerization of aniline in the presence of phytic acid. The resultant NPMCs were demonstrated to be efficient bifunctional catalysts for both the ORR and the oxygen evolution reaction (OER) useful for primary and rechargeable Zn–air batteries.[28] A high open circuit potential (~1.48 V), a large energy density (~835 W h kg_{Zn}^{-1}) and a peak power density (~55 mW cm^{-2}), as well as an excellent durability (over 240 h after recycling two times) were observed for a primary Zn–air battery based on the NPMC metal-free air electrode operating in ambient air with an aqueous KOH electrolyte. Stable 180 cycles at 2 mA cm^{-2} were achieved for a two-electrode rechargeable battery.

Similarly, good stability (600 cycles for 100 h) was obtained for a three-electrode rechargeable battery using two NPMC metal-free air electrodes to separate the ORR and the OER. Theoretical calculation studies showed that the N,P co-doping and graphene edge effects account for good performance and long-term stability of Zn–air batteries.[28] This study indicates that the N and P co-doping and the highly porous network of the carbon foam are critical for both the ORR and the OER (Fig. 9).

Given that Li-ion batteries possess a limited energy density, new types of batteries with higher energy density or more cost-effectiveness, including Na-ion batteries and Li–sulfur batteries, have been recently exploited. Because of their well-defined 3D morphology and porous structure in conjunction with their enhanced electrical conductivity and surface hydrophilicity by heteroatom-doping, 3D N-doped graphene foams have been used as anodes to significantly improve the overall performance of Na-ion batteries, which can maintain a charge capacity of 594 mA h g^{-1} after 150 cycles with 69.7% retention of the initial charge capacity. The above performance significantly outperformed that of previously reported carbonaceous materials. Meanwhile, to overcome the low rate capability and poor cycling life of the

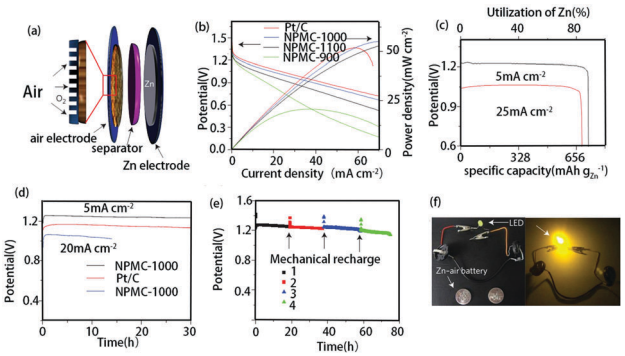

Fig. 9 Performance of a primary Zn–air battery. (a) Schematic of a primary Zn–air battery. (b) Polarization and power density curves of primary Zn–air batteries using Pt/C, NPMC-900, NPMC-1000, and NPMC-1100 as ORR catalysts. (c) Specific capacities of the Zn–air batteries using NPMC-1000 as an ORR catalyst are normalized to the mass of the consumed Zn. (d) Discharge curves of the primary Zn–air batteries using Pt/C and NPMC-1000 as an ORR catalyst and a KOH electrolyte at various current densities. (e) Long-time durability of the primary Zn–air battery using a NPMC-1000 catalyst at a current density of 2 mA cm^{-2}. (f) Optical images of an LED (~2.2 V) before and after being driven by two Zn–air batteries in series. Reprinted from ref. 28 with permission. Copyright 2015, Nature Publishing Group.

lithium–sulfur batteries due to the low conductivities of sulfur and the shuttle effect of the reaction intermediate, Xu *et al.* reported the sulfur edge-functionalized graphene nanoplatlets (SGnPs) prepared by a simple ball-milling technique. It was further found that the edge functionalized SGnPs can be used as a highly efficient cathode electrode for Li–sulfur batteries.[82] The sulfur edge-functionalized GnPs can deliver a high initial reversible capacity of 1265.3 mA h g^{-1} at 0.1 C with an excellent rate capability and a high reversible capacity of 966.1 mA h g^{-1} at 2 C with a low capacity decay rate of 0.099% per cycle over 500 cycles, which outperform the current state-of-the-art cathode materials for lithium–sulfur batteries. These results clearly show that the edge-functionalized GnPs are promising for next generation high-performance lithium–sulfur batteries.

Along with recent development of Li-ion batteries, Na-ion batteries, Li–sulfur batteries and Zn–air batteries, Li–air batteries have also attracted great attention due to their higher energy densities. However, expensive noble metal or noble metal oxide based ORR and OER catalysts are generally needed for metal–air batteries. In this context, metal-free N-doped VACNTs have been demonstrated as effective catalysts for oxygen reduction in a Li–air battery.[67] While 3D N,P-codoped mesoporous carbon foams are effective metal-free bifunctional electrocatalysts for both oxygen reduction and oxygen evolution in high-performance primary and rechargeable Zn–air batteries (*vide supra*).[28] For Li–air batteries, a rationally designed oxygen electrode based on a vertically aligned nitrogen-doped coral-like carbon nanofiber array supported by a piece of stainless steel cloth has been developed, from which a nonaqueous Li–O_2 battery was fabricated to show an energy efficiency as high as 90% and a narrow voltage gap of 0.3 V between discharge/charge plateaus. In the meantime, more than 150 highly reversible cycles under a specific capacity of 1000 mA h g^{-1} was obtained (Fig. 10).[67] These results demonstrate that using a rationally designed carbon-based oxygen electrode

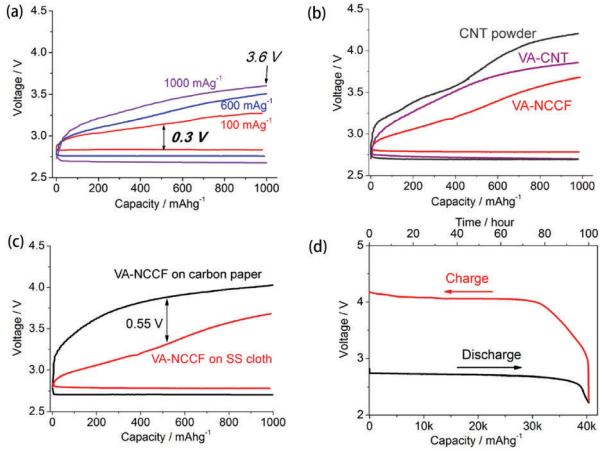

Fig. 10 (a) Rate performance of the VANCCF electrode under current densities of 100, 600, and 1000 mA g^{-1}. (b) Comparison of the VANCCF with undoped vertically aligned carbon nanotubes (VACNTs) and CNT powder. In all cases, a piece of microporous stainless steel cloth was used as the current collector. (c) The VANCCF forest on two different kinds of current collectors: the stainless steel cloth and Toray carbon paper. (d) Discharge/charge voltage profile of the VANCCF as a function of specific capacity. The cutoff voltages were 2.2 V for discharging and 4.4 V for charging. Current density was 500 mA g^{-1}. Reprinted from ref. 67 with permission. Copyright 2014, American Chemical Society.

can be feasible for highly efficient and reversible Li–O_2 batteries. This work may shed light on the research and development of Li–O_2 batteries and other energy devices. Though recent attractive studies show great promise for the application of functionalized CNTs and graphene as efficient electrode materials for energy storage, it is still far away from practical application. There remains much work to do.

4. Conclusions

As can be seen above, CNTs and graphene-based materials are promising for developing the next-generation supercapacitors and batteries for efficient energy storage. However, pristine CNTs and graphene are difficult to be processed into useful forms due to their poor solubility and fusibility. For energy storage applications, therefore, it is highly desirable to functionalize CNTs and graphene. Consequently, various covalent and noncovalent functionalization methods have been developed. In this review article, we have summarized recent progress in the functionalization of CNTs and graphene, by chemical modification, heteroatom-doping, and/or ball milling, for energy storage applications in supercapacitors and batteries. Recent work has clearly shown that functionalized CNTs and graphene-based materials hold great promise as electrode materials in high-performance supercapacitors and batteries. The electrochemical performance of the supercapacitors and batteries based on functionalized CNTs and graphene can be further improved by their self-assembled three-dimensional structures, *via* π–π interactions or CVD fabrication, with a well-defined large-surface-area mesoporous network for efficient charge storage and electron/electrolyte transport. In spite of the fact that various functionalized CNTs and graphene have been developed for energy storage, controlled functionalization of CNTs and graphene with tailor-made structures is still difficult, if not impossible. Besides, it is challenging to precisely locate and characterize the active sites (*e.g.* for ORR or OER) in the functionalized CNTs and graphene. An experimental and theoretical combined approach is needed to better understand the functionalization mechanism and the structure–property relationship for the functionalized CNTs and graphene. Furthermore, it is also important to scale up the production of functionalized CNTs and graphene-based electrode materials at low-cost, particularly the 3D structured carbon nanomaterials, and to meet the requirements of portable and wearable optoelectronics with integrated self-powering systems. Nevertheless, the present review article has clearly demonstrated that carbon nanomaterials with controllable 3D structures are promising electrode materials for efficient energy storage. Continued research in this field should lead to revolutionized renewable energy technologies.

Competing interests

The authors declare that they have no competing interests.

Acknowledgements

We are grateful for the financial support from the U.S. Department of Defense Multidisciplinary University Initiative under AFOSR (FA9550-12-1-0037; J. Harrison, Program Manager), Natural Science Foundation of China (No. 21401177 and 21501160), and the ''1000 plan'' from the Chinese Government.

Notes and references

1 L. Dai, *Acc. Chem. Res.*, 2013, **46**, 31–42.
2 L. Qu, Y. Liu, J.-B. Baek and L. Dai, *ACS Nano*, 2010, **4**, 1321–1326.
3 F. Du, D. Yu, L. Dai, S. Ganguli, V. Varshney and A. K. Roy, *Chem. Mater.*, 2011, **23**, 4810–4816.
4 J.-M. Tarascon and M. Armand, *Nature*, 2001, **414**, 359–367.
5 I.-Y. Jeon, H.-J. Choi, M. Choi, J.-M. Seo, S.-M. Jung, M.-J. Kim, S. Zhang, L. Zhang, Z. Xia, L. Dai, N. Park and J.-B. Baek, *Sci. Rep.*, 2013, **3**, 1810–1816.
6 P. Simon, Y. Gogotsi and B. Dunn, *Science*, 2014, **343**, 1210–1211.
7 R. V. Noorden, *Nature*, 2014, **507**, 26–28.
8 P. Simon and Y. Gogotsi, *Nat. Mater.*, 2008, **7**, 845–854.
9 J. L. Cheng, B. Wang, Y. P. Wu, D. Wang and D. N. He, *Electrochem. Commun.*, 2012, **23**, 5–8.
10 B. Wang, J. Cheng, Y. Wu, D. Wang and D. He, *J. Mater. Chem. A*, 2013, **1**, 1368–1373.
11 I.-Y. Jeon, M. J. Ju, J. Xu, H.-J. Choi, J.-M. Seo, M.-J. Kim, I. T. Choi, H. M. Kim, J. C. Kim, J.-J. Lee, H. K. Liu, H. K. Kim, S. Dou, L. Dai and J.-B. Baek, *Adv. Funct. Mater.*, 2015, **25**, 1170–1179.
12 J. Cheng, H. Xin, H. Zheng and B. Wang, *J. Power Sources*, 2013, **232**, 152–158.
13 J. Cheng, B. Wang, H. L. Xin, G. Yang, H. Cai, F. Nie and H. Huang, *J. Mater. Chem. A*, 2013, **1**, 10814–10820.
14 D. Yuan, J. Cheng, G. Qu, X. Li, W. Ni, B. Wang and H. Liu, *J. Power Sources*, 2016, **301**, 131–137.
15 I. H. Son, J. H. Park, S. Kwon, S. Park, M. H. Rümmeli, A. Bachmatiuk, H. J. Song, J. Ku, J. W. Choi, J. Choi, S.-G. Doo and H. Chang, *Nat. Commun.*, 2015, **6**, 7393–7400.
16 J. Xu, Y. Chen and L. Dai, *Nat. Commun.*, 2015, **6**, 8103–8112.
17 L. Dai, D. W. Chang, J.-B. Baek and W. Lu, *Small*, 2012, **8**, 1130–1166.
18 J. Cheng, L. Huang, X. Li, D. Yuan, W. Ni, G. Qu, Q. Guan, Y. Zhang and B. Wang, *J. Mater. Chem. A*, 2015, **3**, 4049–4057.

19 J. Zhao, Z. Lu, H. Wang, W. Liu, H.-W. Lee, K. Yan, D. Zhuo, D. Lin, N. Liu and Y. Cui, *J. Am. Chem. Soc.*, 2015, **137**, 8372–8375.
20 Q. Sun, X. Fang, W. Weng, J. Deng, P. Chen, J. Ren, G. Guan, M. Wang and H. Peng, *Angew. Chem., Int. Ed.*, 2015, **54**, 10685–10690.
21 X. Fang, W. Weng, J. Ren and H. Peng, *Adv. Mater.*, 2016, **28**, 491–496.
22 A. Manthiram, S.-H. Chung and C. Zu, *Adv. Mater.*, 2015, **27**, 1980–2006.
23 G. Zhou, E. Paek, G. Hwang and A. Manthiram, *Nat. Commun.*, 2015, **6**, 7760–7771.
24 L. Huang, J. Cheng, G. Qu, X. Li, Y. Hu, W. Ni, D. Yuan, Y. Zhang and B. Wang, *RSC Adv.*, 2015, **5**, 23749–23757.
25 G. Qu, J. Cheng, X. Li, D. Yuan, P. Chen, X. Chen, B. Wang and H. Peng, *Adv. Mater.*, 2016, **28**, 3646–3652.
26 Y. Xu, Y. Zhang, Z. Guo, J. Ren, Y. Wang and H. Peng, *Angew. Chem., Int. Ed.*, 2015, **54**, 15390–15394.
27 M. Xu, D. G. Ivey, Z. Xie and W. Qu, *J. Power Sources*, 2015, **283**, 358–371.
28 J. Zhang, Z. Zhao, Z. Xia and L. Dai, *Nat. Nanotechnol.*, 2015, **10**, 444–452.
29 R. Black, B. Adams and L. F. Nazar, *Adv. Energy Mater.*, 2012, **2**, 801–815.
30 J.-S. Lee, S. Tai Kim, R. Cao, N.-S. Choi, M. Liu, K. T. Lee and J. Cho, *Adv. Energy Mater.*, 2011, **1**, 34–50.
31 J. Hassoun, H.-G. Jung, D.-J. Lee, J.-B. Park, K. Amine, Y.-K. Sun and B. Scrosati, *Nano Lett.*, 2012, **12**, 5775–5779.
32 T. Zhang and H. Zhang, *Nat. Commun.*, 2013, **4**, 1817–1824.
33 K. Gong, F. Du, Z. Xia, M. Durstock and L. Dai, *Science*, 2009, **323**, 760–764.
34 P. G. Bruce, L. J. Hardwick and K. M. Abraham, *MRS Bull.*, 2011, **36**, 506–512.
35 Y. Li and H. Dai, *Chem. Soc. Rev.*, 2014, **43**, 5257–5275.
36 D. Kundu, E. Talaie, V. Duffort and L. F. Nazar, *Angew. Chem., Int. Ed.*, 2015, **54**, 3431–3448.
37 N. Zhao, G. Wang, Y. Huang, B. Wang, B. Yao and Y. Wu, *Chem. Mater.*, 2008, **20**, 2612–2614.
38 R. Saito, M. Fujita, G. Dresselhaus and M. S. Dresselhaus, *Appl. Phys. Lett.*, 1992, **60**, 2204–2206.
39 L. Dai, A. Patil, X. Gong, Z. Guo, L. Liu, Y. Liu and D. Zhu, *ChemPhysChem*, 2003, **4**, 1150–1169.
40 R. Baughman, A. Zakhidov and W. de Heer, *Science*, 2002, **297**, 787–792.
41 H. Chen, A. Roy, J.-B. Baek, L. Zhu, J. Qu and L. Dai, *Mater. Sci. Eng., R*, 2010, **70**, 63–91.
42 J. Lee, I. Y. Stein, S. S. Kessler and B. L. Wardle, *ACS Appl. Mater. Interfaces*, 2015, **7**, 8900–8905.
43 C.-M. Seah, S.-P. Chai and A. R. Mohamed, *Carbon*, 2011, **49**, 4613–4635.
44 G. D. Nessim, A. J. Hart, J. S. Kim, D. Acquaviva, J. Oh, C. D. Morgan, M. Seita, J. S. Leib and C. V. Thompson, *Nano Lett.*, 2008, **8**, 3587–3593.
45 Z. Yang, X. Zhu, X. Huang, Y. Cheng, Y. Liu, H. Geng, Y. Wu, Y. Su, H. Wei and Y. Zhang, *Nanoscale Res. Lett.*, 2013, **8**, 501.
46 W. Lü, J. Dong and Z.-Y. Li, *Phys. Rev. B: Condens. Matter Mater. Phys.*, 2000, **63**, 033401.
47 S. Esconjauregui, R. Xie, M. Fouquet, R. Cartwright, D. Hardeman, J. Yang and J. Robertson, *J. Appl. Phys.*, 2013, **113**, 144309.
48 B. Liu, C. Wang, J. Liu, Y. Che and C. Zhou, *Nanoscale*, 2013, **5**, 9483–9502.
49 X. Sun, T. Chen, Z. Yang and H. Peng, *Acc. Chem. Res.*, 2013, **46**, 539–549.
50 Z. Li, Z. Liu, H. Sun and C. Gao, *Chem. Rev.*, 2015, **115**, 7046–7117.
51 B. Wang, H. Xin, X. Li, J. Cheng, G. Yang and F. Nie, *Sci. Rep.*, 2014, **4**, 3729–3735.
52 J. Cheng, B. Wang, H. L. Xin, C. Kim, F. Nie, X. Li, G. Yang and H. Huang, *J. Mater. Chem. A*, 2014, **2**, 2701–2707.
53 J. Cheng, B. Wang, C.-M. Park, Y. Wu, H. Huang and F. Nie, *Chem. – Eur. J.*, 2013, **19**, 9866–9874.
54 S. Takenaka, H. Miyamoto, Y. Utsunomiya, H. Matsune and M. Kishida, *J. Phys. Chem. C*, 2014, **118**, 774–783.
55 A. K. Geim and K. S. Novoselov, *Nat. Mater.*, 2007, **6**, 183–191.
56 K. S. Novoselov, A. K. Geim, S. V. Morozov, D. Jiang, M. I. Katsnelson, I. V. Grigorieva, S. V. Dubonos and A. A. Firsov, *Nature*, 2005, **438**, 197–200.
57 S. Eigler and A. Hirsch, *Angew. Chem., Int. Ed.*, 2014, **53**, 7720–7738.
58 V. Schwartz, W. Fu, Y.-T. Tsai, H. M. Meyer, A. J. Rondinone, J. Chen, Z. Wu, S. H. Overbury and C. Liang, *ChemSusChem*, 2013, **6**, 840–846.
59 D. Tasis, N. Tagmatarchis, A. Bianco and M. Prato, *Chem. Rev.*, 2006, **106**, 1105–1136.
60 G. Gu, J. Cheng, X. Li, W. Ni, Q. Guan, G. Qu and B. Wang, *J. Mater. Chem. A*, 2015, **3**, 6642–6648.
61 Q. Cheng, B. Wang, C. Zhang and Z. Liang, *Small*, 2010, **6**, 763–767.
62 P. Tamilarasan and S. Ramaprabhu, *J. Mater. Chem. A*, 2014, **2**, 14054–14063.
63 J. C. Bachman, R. Kavian, D. J. Graham, D. Y. Kim, S. Noda, D. G. Nocera, Y. Shao-Horn and S. W. Lee, *Nat. Commun.*, 2015, **6**, 7040–7048.
64 X. Fan, C. Yu, Z. Ling, J. Yang and J. Qiu, *ACS Appl. Mater. Interfaces*, 2013, **5**, 2104–2110.
65 J. Shui, M. Wang, F. Du and L. Dai, *Sci. Adv.*, 2015, **1**, e1400129.
66 L. Dai, Y. Xue, L. Qu, H. J. Choi and J. B. Baek, *Chem. Rev.*, 2015, **115**, 4823–4892.
67 J. Shui, F. Du, C. Xue, Q. Li and L. Dai, *ACS Nano*, 2014, **8**, 3015–3022.
68 A. Hirsch, *Angew. Chem., Int. Ed.*, 2002, **41**, 1853–1859.
69 R. Zhang, S. He, Y. Lu and W. Chen, *J. Mater. Chem. A*, 2015, **3**, 3559–3567.
70 Y. Cheng, P. K. Shen and S. P. Jiang, *Int. J. Hydrogen Energy*, 2014, **39**, 20662–20670.
71 J. Liu, A. Shen, X. Wei, K. Zhou, W. Chen, F. Chen, J. Xu, S. Wang and L. Dai, *ACS Appl. Mater. Interfaces*, 2015, **7**, 20507–20512.
72 R. Kumar, R. K. Singh, P. K. Dubey, D. P. Singh, R. M. Yadav and R. S. Tiwari, *Adv. Mater. Interfaces*, 2015, **2**, 201500191.
73 L. Zhang, C. M. B. Holt, E. J. Luber, B. C. Olsen, H. Wang, M. Danaie, X. Cui, X. Tan, V. W. Lui, W. P. Kalisvaart and D. Mitlin, *J. Phys. Chem. C*, 2011, **115**, 24381–24393.
74 E. Cunha, M. F. Proença, F. Costa, A. J. Fernandes, M. A. C. Ferro, P. E. Lopes, M. González-Debs, M. Melle-Franco, F. L. Deepak and M. C. Paiva, *ChemistryOpen*, 2015, **4**, 115–119.
75 A. Mandal and A. K. Nandi, *J. Phys. Chem. C*, 2012, **116**, 9360–9371.
76 J. Liu, Y. Xue, Y. Gao, D. Yu, M. Durstock and L. Dai, *Adv. Mater.*, 2012, **24**, 2228–2233.
77 D. Yu, Y. Yang, M. Durstock, J.-B. Baek and L. Dai, *ACS Nano*, 2010, **4**, 5633–5640.
78 J. Liu, Y. Xue and L. Dai, *J. Phys. Chem. Lett.*, 2012, **3**, 1928–1933.
79 D. Yu, K. Park, M. Durstock and L. Dai, *J. Phys. Chem. Lett.*, 2011, **2**, 1113–1118.
80 J. Xu, M. Wang, N. P. Wickramaratne, M. Jaroniec, S. Dou and L. Dai, *Adv. Mater.*, 2015, **27**, 2042–2048.
81 S. Wang, L. Zhang, Z. Xia, A. Roy, D. W. Chang, J.-B. Baek and L. Dai, *Angew. Chem., Int. Ed.*, 2012, **51**, 4209–4212.
82 J. Xu, J. Shui, J. Wang, M. Wang, H. Liu, S. Dou, I.-Y. Jeon, J.-M. Seo, J.-B. Baek and L. Dai, *ACS Nano*, 2014, **8**, 10920–10930.
83 Z. Ma, S. Dou, A. Shen, L. Tao, L. Dai and S. Wang, *Angew. Chem., Int. Ed.*, 2015, **54**, 1888–1892.
84 M.-J. Kim, I.-Y. Jeon, J.-M. Seo, L. Dai and J.-B. Baek, *ACS Nano*, 2014, **8**, 2820–2825.
85 I.-Y. Jeon, Y.-R. Shin, G.-J. Sohn, H.-J. Choi, S.-Y. Bae, J. Mahmood, S.-M. Jung, J.-M. Seo, M.-J. Kim, D. Wook Chang, L. Dai and J.-B. Baek, *Proc. Natl. Acad. Sci. U. S. A.*, 2012, **109**, 5588–5593.
86 I.-Y. Jeon, H.-J. Choi, S.-M. Jung, J.-M. Seo, M.-J. Kim, L. Dai and J.-B. Baek, *J. Am. Chem. Soc.*, 2013, **135**, 1386–1393.
87 E.-K. Choi, I.-Y. Jeon, S.-Y. Bae, H.-J. Lee, H. S. Shin, L. Dai and J.-B. Baek, *Chem. Commun.*, 2010, **46**, 6320–6322.
88 I.-Y. Jeon, H.-J. Choi, M. J. Ju, I. T. Choi, K. Lim, J. Ko, H. K. Kim, J. C. Kim, J.-J. Lee, D. Shin, S.-M. Jung, J.-M. Seo, M.-J. Kim, N. Park, L. Dai and J.-B. Baek, *Sci. Rep.*, 2013, **3**, 2260–2266.
89 J. Xu, I.-Y. Jeon, J.-M. Seo, S. Dou, L. Dai and J.-B. Baek, *Adv. Mater.*, 2014, **26**, 7317–7323.
90 Z. Xiang, Q. Dai, J. F. Chen and L. Dai, *Adv. Mater.*, 2016, **28**, 6253–6261.
91 W. Lu, L. Qu, K. Henry and L. Dai, *J. Power Sources*, 2009, **189**, 1270–1277.
92 D. Yu and L. Dai, *J. Phys. Chem. Lett.*, 2010, **1**, 467–470.
93 H. Jiang, C. Li, T. Sun and J. Ma, *Nanoscale*, 2012, **4**, 807–812.
94 Q. Guan, J. Cheng, B. Wang, W. Ni, G. Gu, X. Li, L. Huang, G. Yang and F. Nie, *ACS Appl. Mater. Interfaces*, 2014, **6**, 7626–7632.

95 G. Zheng, L. Hu, H. Wu, X. Xie and Y. Cui, *Energy Environ. Sci.*, 2011, **4**, 3368–3373.
96 T. Chen and L. Dai, *Energy Storage Mater.*, 2016, **2**, 21–26.
97 X.-C. Dong, H. Xu, X.-W. Wang, Y.-X. Huang, M. B. Chan-Park, H. Zhang, L.-H. Wang, W. Huang and P. Chen, *ACS Nano*, 2012, **6**, 3206–3213.
98 C. Yuan, L. Yang, L. Hou, J. Li, Y. Sun, X. Zhang, L. Shen, X. Lu, S. Xiong and X. W. Lou, *Adv. Funct. Mater.*, 2012, **22**, 2560–2566.
99 P. Yang, L. Du, X. Yu, P. Liu, J. Song and W. Mai, *J. Mater. Chem. A*, 2014, **2**, 17561–17567.
100 Z. Zhang, J. Deng, X. Li, Z. Yang, S. He, X. Chen, G. Guan, J. Ren and H. Peng, *Adv. Mater.*, 2015, **27**, 356–362.
101 S. Pan, J. Deng, G. Guan, Y. Zhang, P. Chen, J. Ren and H. Peng, *J. Mater. Chem. A*, 2015, **3**, 6286–6290.
102 Y. Qiu, G. Li, Y. Hou, Z. Pan, H. Li, W. Li, M. Liu, F. Ye, X. Yang and Y. Zhang, *Chem. Mater.*, 2015, **27**, 1194–1200.
103 T. Chen, Y. Xue, A. K. Roy and L. Dai, *ACS Nano*, 2014, **8**, 1039–1046.
104 Y. Ma, P. Li, J. W. Sedloff, X. Zhang, H. Zhang and J. Liu, *ACS Nano*, 2015, **9**, 1352–1359.
105 Y. Xue, L. Zhu, H. Chen, J. Qu and L. Dai, *Carbon*, 2015, **92**, 305–310.
106 N. A. Kumar, H.-J. Choi, Y. R. Shin, D. W. Chang, L. Dai and J.-B. Baek, *ACS Nano*, 2012, **6**, 1715–1723.
107 Y. Xue, H. Chen, J. Qu and L. Dai, *2D Mater.*, 2015, **2**, 04401.
108 T. Chen, H. Peng, M. Durstock and L. Dai, *Sci. Rep.*, 2014, **4**, 3612.
109 T. Chen, R. Hao, H. Peng and L. Dai, *Angew. Chem., Int. Ed.*, 2015, **54**, 618–622.
110 Y. Xue, Y. Ding, J. Niu, Z. Xia, A. Roy, H. Chen, J. Qu, Z. Wang and L. Dai, *Sci. Adv.*, 2015, **1**, 1400198–1400207.
111 D. N. Futaba, K. Hata, T. Yamada, T. Hiraoka, Y. Hayamizu, Y. Kakudate, O. Tanaike, H. Hatori, M. Yumura and S. Iijima, *Nat. Mater.*, 2006, **5**, 987–994.
112 H. Zhang, G. Cao, Z. Wang, Y. Yang, Z. Shi and Z. Gu, *Nano Lett.*, 2008, **8**, 2664–2668.
113 X. Li, X. Li, J. Cheng, D. Yuan, W. Ni, Q. Guan, L. Gao and B. Wang, *Nano Energy*, 2016, **21**, 228–237.
114 J. Xu, Y. Lin, J. W. Connell and L. Dai, *Small*, 2015, **11**, 6179–6185.
115 J. Zhang, Z. Xia and L. Dai, *Sci. Adv.*, 2015, **1**, e1500564.
116 G. Qu, J. Cheng, X. Li, L. Huang, W. Ni, Z. Wang and B. Wang, *ACS Appl. Mater. Interfaces*, 2015, **7**, 16668–16675.